Liu, Xiaolong; Radfar, Behrad; Chen, Kexun; Pälikkö, Elmeri; Pasanen, Toni; Vähänissi, Ville; Savin, Hele

Millisecond-Level Minority Carrier Lifetime in Femtosecond Laser-Textured Black Silicon

Published in:
IEEE Photonics Technology Letters

DOI:
10.1109/LPT.2022.3190270

Published: 15/08/2022

Document Version
Publisher's PDF, also known as Version of record

Millisecond-Level Minority Carrier Lifetime in Femtosecond Laser-Textured Black Silicon

Xiaolong Liu, Behrad Radfar, *Graduate Student Member, IEEE*, Kexun Chen, Elmeri Pälikkö, Toni P. Pasanen, Ville Vähänissi, and Hele Savin

***Abstract*— Femtosecond laser-textured black silicon (fs-bSi) is known to suffer from heavy minority carrier recombination resulted from laser irradiation. In this letter, we demonstrate that the thermal annealing step, generally used to recover the crystal damage, could improve the minority carrier lifetime of the fs-bSi wafers only from 8 μs to 12 μs, even when using as high temperature as 800 °C. However, with an optimized wet chemical etching process, we obtain a high minority carrier lifetime of 2 ms without sacrificing the optical properties of the samples, i.e., the absorptance remains above 90% in the studied wavelength range (250–1100 nm). Increasing the etching time further leads to a total recovery of the lifetime up to 10.5 ms, which proves that the damage originating from the fs-laser texturing extends only to the near-surface layer (a few μm) of silicon.**

***Index Terms*— Annealing, black silicon, charge carrier lifetime, etch back, fs-laser, recombination, silicon.**

I. Introduction

FEMTOSECOND laser-textured black silicon (fs-bSi) holds great promise in optoelectronic applications such as photovoltaics and photodetection due to its ability to absorb light efficiently over a wide spectral range [1]–[3] combined with the possibility to simultaneously form a p-n junction using hyperdoping [4], [5]. One of the major challenges, on the other hand, is the carrier recombination induced by the laser processing, which originates from the introduction of various types of defects and contaminants [6], [7]. As a result, even with an efficient surface passivation layer, the fs-bSi shows a low minority carrier lifetime [8], which is known to harm the optoelectronic device performance.

Attempts have been made to recover the laser induced damage by using high-temperature thermal annealing [7], [9], [10]. Raman spectroscopy measurements have indicated that the crystallinity can be substantially improved at the annealing temperature of 700 °C [7]. However, such a measurement does not necessarily correlate with carrier recombination; thus, the recovery of crystallinity cannot guarantee an improvement in the minority carrier lifetime. Therefore, a direct measurement of the carrier lifetime from the fs-bSi samples would be preferred to estimate the remaining amount of damage from the laser processing. An additional benefit of measuring carrier lifetime over crystallinity is that the minority carrier lifetime measurements also reveal other sources of recombination [11], [12] resulting from, e.g., the laser processing.

Manuscript received 29 April 2022; revised 20 June 2022; accepted 8 July 2022. Date of publication 12 July 2022; date of current version 3 August 2022. This work was supported in part by the Business Finland through "FemtoBlack" under Grant 7479/31/2019, in part by the Academy of Finland under Grant 331313, in part by the Finnish Research Impact Foundation, and in part by the European Metrology Programme for Innovation and Research (EMPIR) co-financed by the Participating States and from the European Union's Horizon 2020 Research and Innovation Program through "NanoWires" under Grant 19ENG05. *(Corresponding author: Xiaolong Liu.)*

The authors are with the Department of Electronics and Nanoengineering, Aalto University, 02150 Espoo, Finland (e-mail: xiaolong.liu@aalto.fi).

Color versions of one or more figures in this letter are available at https://doi.org/10.1109/LPT.2022.3190270.

Digital Object Identifier 10.1109/LPT.2022.3190270

Post-laser etching, such as the chemical etching of the surface layer, could be an alternative method for high-temperature annealing, as it has been shown to provide a simple and effective means to improve the carrier lifetime of the laser irradiated silicon [13], [14]. However, earlier studies on such a post-etching approach on bSi fabricated by metal-assisted chemical etching (MACE) [15] or reactive ion etching (RIE) [16] have shown a trade-off between lifetime and optical properties. Therefore, it is worth investigating if the lifetime in the fs-bSi can be increased by the post-etching without too much deteriorating the optical properties.

In this letter, we examine the carrier recombination of fs-bSi samples using direct minority carrier lifetime measurement methods such as the transient photoconductance decay (PCD) and the quasi-steady-state photoconductance (QSSPC) [17] techniques for injection dependent lifetime measurement of high-lifetime and low-lifetime samples, respectively, and quasi-steady-state microwave detected photoconductance decay (QSS-μPCD) technique for lifetime mapping [18]. We first investigate whether the conventional thermal annealing could improve the carrier lifetime of the fs-bSi wafers, using a relatively high temperature of 800 °C that has been shown to significantly improve the silicon crystallinity and that already exceeds the optimal annealing temperature to obtain the maximum device responsivity [4], [5]. Then, we study how the minority carrier lifetime is affected by the etching of the fs-bSi surface layers by an acidic solution with different durations. During the etching process, we also aim to minimize the losses on optical absorptance resulting from the possible change in surface structures.

II. Post-Laser Thermal Annealing

To begin with, 4-inch boron-doped FZ-Si wafers ((100), 3 Ω cm, 280 μm) were used as the substrate. A circular bSi area with a diameter of 4 cm was fabricated at the center of the wafer under the fs-laser fluence of 5.4 kJ m^{-2} with the detailed experimental procedures described elsewhere [8], whereas the non-lasered planar area on the same wafer served as a reference. Subsequently, both front and rear surfaces were passivated by atomic layer deposited (ALD) Al_2O_3 and annealed at 400 °C (30 min, N_2 ambient) to activate the passivation [8]. Fig. 1 shows the injection-dependent carrier lifetime (denoted by effective lifetime, τ_{eff}) from this wafer

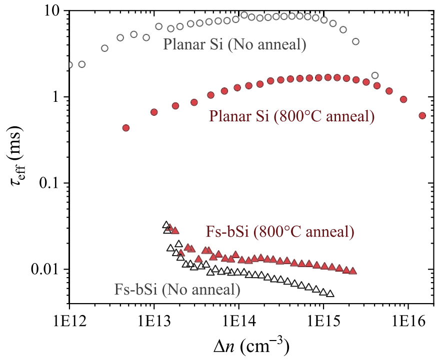

Fig. 1. The effective minority carrier lifetime (τ_{eff}) as a function of the injection level (or excess carrier density, Δn) on fs-bSi and planar areas before and after high temperature (800 °C) annealing. Note the logarithmic scales.

measured both on the bSi area as well as on the planar reference areas. As seen, the bSi area (open triangles) shows a low lifetime of $\sim$8 μs at the excess carrier density (Δn) of 1.0E15 cm^{-3} (the lifetime values below are reported at the same Δn) which indicates heavy carrier recombination after the laser processing. A high lifetime of $\sim$10 ms was measured from the planar area (open circles), which is expected from the well surface passivated Si wafer [19].

Then, we fabricated another similar fs-bSi sample to study the effect of the high-temperature annealing on the minority carrier lifetime. Prior to the surface passivation, the wafer was annealed at 800 °C (30 min, N_2 ambient) and cleaned by the standard RCA cleaning process before and after annealing; otherwise, the process was identical. Quite surprisingly, only a small improvement in lifetime is seen from the bSi area ($\sim$12 μs) as shown in Fig. 1 (red triangles). As a reference, the lifetime in the planar Si area drops to $\sim$1.5 ms (red circles) after annealing, which indicates some contamination from the furnace. However, considering the large difference (>100 times) in lifetime between the bSi and the planar Si areas, the low lifetime measured in the bSi after annealing is not due to the contamination but shows clearly that such an annealing step is not enough to reduce the laser-induced recombination. This result indicates that most lifetime limiting laser-induced defects are thermally stable at least up to 800 °C. Further increasing the annealing temperature could bring many drawbacks, such as metal contamination [11], [12] and dopant diffusion [20], [21]. Thus, it seems not possible to recover the lifetime of laser-textured Si by solely relying on thermal annealing.

III. Post-Laser Chemical Etching

Next, we study if we can impact the minority carrier lifetime in the fs-bSi samples by post-laser chemical etching. Several identical wafers consisting of fs-bSi areas with different laser fluence were fabricated with the layout shown in Fig. 2(a). The laser-processed wafers were immersed in an acid based etching solution [HF(50%):HNO_3(69%):H_2O = 1:2:2, v:v:v] adapted from Ref. [22] with varying time durations, t, from 0 (non-etched) to 90 s. The etching rate was $\sim$100 nm/s as determined from a planar Si wafer, based on which the etching depths in the following are estimated.

Fig. 2(b) shows the minority carrier lifetime maps of the samples with the increasing etching time. Clearly, the non-etched reference sample has much lower lifetime in bSi than in planar areas, agreeing with Fig.1. By following the maps to the right, we can observe that the lifetime gradually increases in bSi areas with increasing etching time. After 30 s etching the difference in the lifetime can hardly be observed. Fig. 2(c) presents the same lifetime data as a function of the injection level measured from the bSi area fabricated with the highest fluence. Similar to the maps, after 30 s etching, the bSi area has nearly the same lifetime as that from the planar Si area. These results indicate that it is indeed possible to obtain a high lifetime in fs-bSi and that the laser-induced defects are not located deep inside the substrate.

The laser fluence has some impact also on the amount and the depth of the laser-induced damage, as under the same etching time, higher lifetime was observed on bSi areas with lower fluence. However, the bSi areas fabricated with different fluences have a similar trend, i.e., higher lifetime is observed with increasing etching time.

In addition to the carrier recombination, it is important to also characterize the possible changes in the optical properties of the bSi area. Fig. 2(d) shows the change of the optical absorptance in the range of 250–1100 nm during the etching process. The absorptance spectrum decreases monotonously with increasing etching time most likely due to the change in the surface morphology. Fig. 2(e) summarizes the dependence of the minority carrier lifetime and the absorptance on the etching time. There is an apparent trade-off between the lifetime and the absorptance with the increasing etching time. Based on the results, a 10 s etching seems optimal as simultaneously a high lifetime of 2 ms and a relatively high absorptance of 90.5% are obtained.

It is worth noticing that after etching for 5 s, the absorptance is only slightly reduced in the wavelength range of 250–500 nm, while the rest of the absorptance spectrum remains virtually constant. Meanwhile, the minority carrier lifetime has been increased already by a factor of $\sim$3.9, or the total recombination rate ($1/\tau_{\text{eff}}$) has been decreased by $\sim$74.4% compared to that in the non-etched fs-bSi. This result indicates that heavy recombination occurs at the outmost surface layer in the first $\sim$500 nm. After the 10 s etching, the minority carrier lifetime reaches ms-level, corresponding to a decrease of 99.6% in the total recombination rate compared to that in the non-etched fs-bSi. This means that the damaged structures contributing to the carrier recombination follow a gradient distribution under the fs-bSi surface. The remaining damaged structures contributing to only $\sim$0.4% of the total recombination rate are located roughly between 1 and 9 μm in depth, and the bulk lifetime deeper (>$\sim$9 μm) inside the Si wafer is not affected by the laser texturing at all.

Finally, we characterize the evolution of surface morphology as a function of the etching time. Fig. 3(a–f) shows that with increasing etching time, the surface of the spike-like periodic microstructures becomes smoother, and the silicon bulk is gradually exposed. The gradual smoothing of the surface structures accounts for the decreased absorptance, whereas the removal of surface defected layers contributes mostly to the increased lifetime. In addition, it is observed that the surface area decreases with increased etching time. However, the surface recombination is not limiting the lifetime here, as effectively reduced surface recombination by our

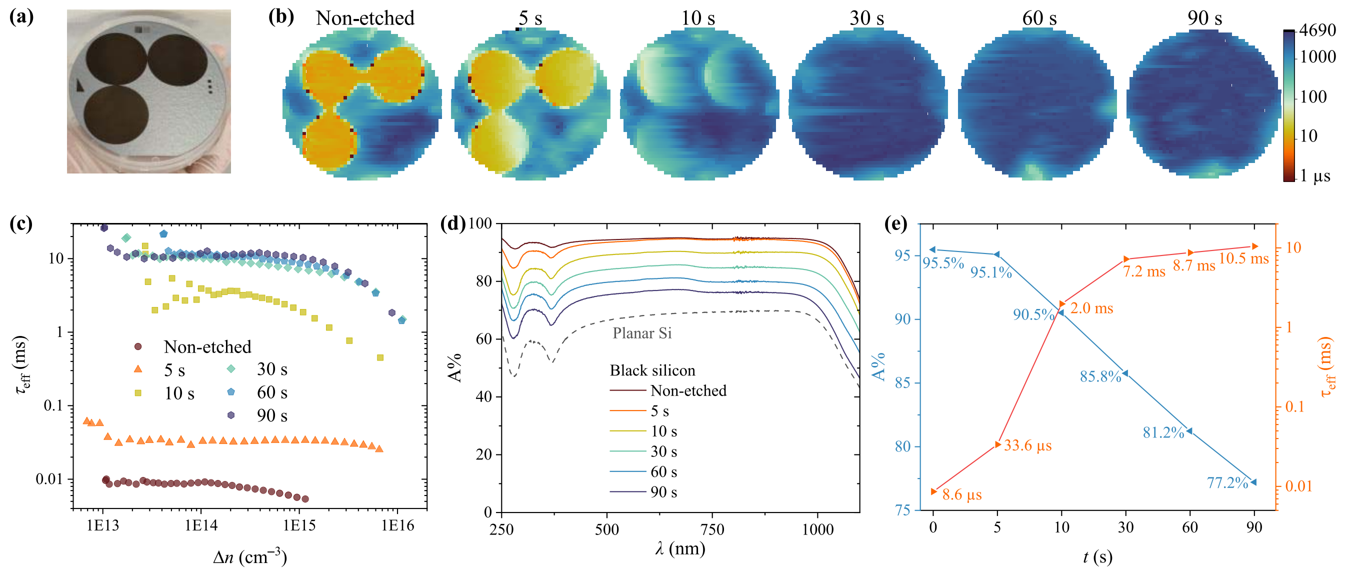

Fig. 2. (a) An optical photograph of a laser-textured wafer (dark circles in upper-left, upper-right, and lower-left correspond to laser fluence of 5.4, 4.3, and 3.2 kJ m^{-2}, respectively). (b) QSS-μPCD lifetime maps with different etching time, t. (c) Injection dependent minority carrier lifetime, τ_{eff}, and (d) optical absorptance, A%, measured from acid-etched fs-bSi wafers with different t. (e) Etching time dependence of the maximum absorptance in the wavelength range of 250–1100 nm and the effective minority carrier lifetime at the excess carrier density of 1.0E15 cm^{-3}. (c)–(e) are measured from areas with the highest fluence.

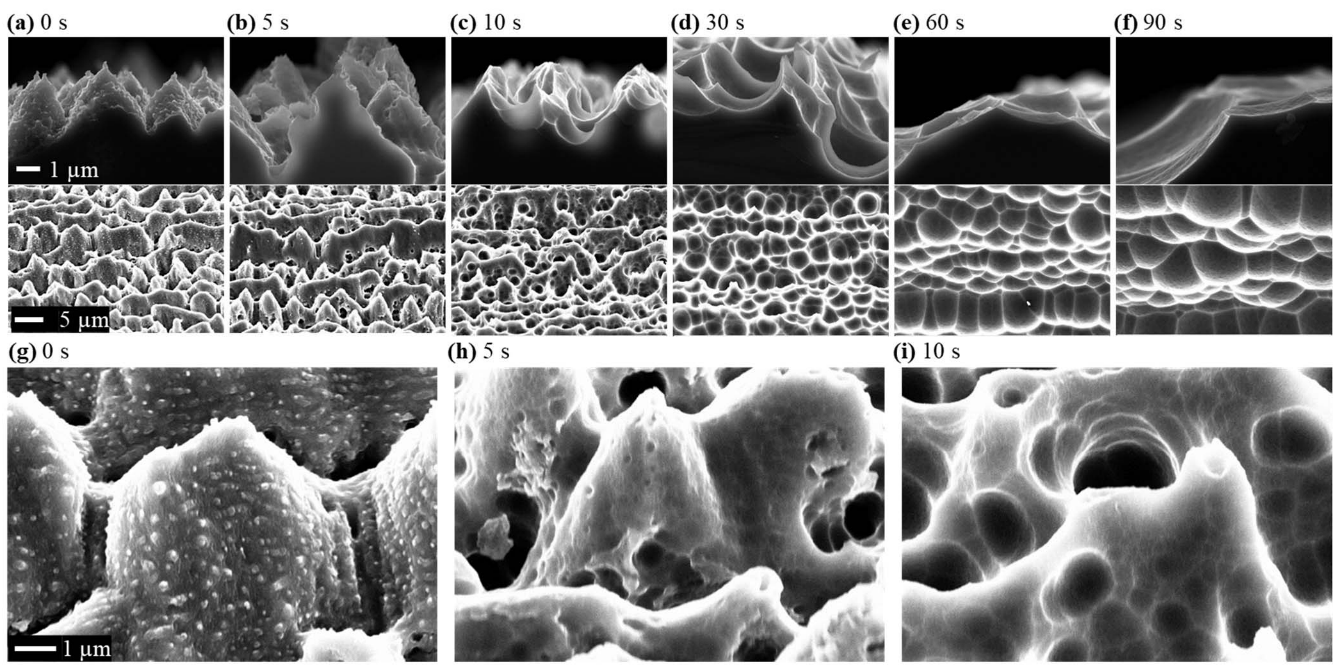

Fig. 3. Cross-sectional (1st row) and 45°-tilt (2nd and 3rd rows) scanning electron microscopic images of fs-bSi samples after different etching time.

ALD Al_2O_3 surface passivation layer has been verified on defect-free bSi structures [22], [23]. Higher magnification in Fig. 3(g–h) shows that the surface nanoparticles are already removed at the initial phase (5 s) of the etching process. This is consistent with the observed drop in absorptance in shorter wavelengths, as it is reported that Si nanostructures enhance the optical absorption at wavelengths below 600 nm [24]. It is worth mentioning that the original height of the microstructures is about 3–5 μm as observed in Fig. 3(a), whereas for the optimized etching time of 10 s, the estimated etching depth is ~1 μm, which corresponds to the observations seen in Fig. 3(c) and 3(i) where most of the microstructures are still present. Another interesting observation is that a full recovery of the lifetime is seen only after etching ~9 μm in depth, which means the laser damage extends somewhat deeper than the height of the original surface texture.

Here, the investigation was based on our previously optimized laser parameters [8] that are similar to what is generally used to create the fs-bSi with high optical absorption in a wide wavelength range. Our results thus indicate that the challenges hindering the application of such highly light-absorptive fs-bSi reside mainly near the surface layer. Compared to rather complicated high-temperature annealing, the post-etching solution developed here should be relatively easy to implement in the actual devices. Furthermore, it would be interesting to test if the post-etching process significantly improves the minority carrier lifetime in hyperdoped fs-bSi as well. Typically, the fs-laser hyperdoping is done together with bSi formation. In this case the doping profile is mainly determined by laser processing parameters, whereas if it was done afterwards, the doping profile would be affected by the surface morphology, similarly as reported in [25], [26].

IV. Conclusion

In conclusion, we demonstrate that thermal annealing at 800°C cannot cure the recombination-active defects in fs-bSi wafers. Instead, we show that the chemical acid-etching after laser processing is an effective method to remove the laser damage and significantly improve the minority carrier lifetime even to ms-level when combined with an ALD Al_2O_3 surface passivation layer. This letter also proves that the most heavily laser-damaged area extends to only a few μm under the fs-bSi surface. Due to the change in surface morphology, the absorptance drops with increasing etching time, which means there is a trade-off between the optical and the electrical properties. Nevertheless, with an optimized etching time, a simultaneously high carrier lifetime of 2 ms and a high absorptance of 90.5% from the surface-modified fs-bSi wafer were obtained. These results set premises for future optoelectronic applications.

Acknowledgment

The authors acknowledge the provision of facilities and technical support by Micronova Nanofabrication Centre and Nanomicroscopy Centre in Espoo, Finland within the OtaNano research infrastructure at Aalto University. The work is related to the Flagship on Photonics Research and Innovation "PREIN" funded by Academy of Finland.

References

[1] J. M. Warrender, "Laser hyperdoping silicon for enhanced infrared optoelectronic properties," *Appl. Phys. Rev.*, vol. 3, Jul. 2016, Art. no. 031104, doi: 10.1063/1.4960752.

[2] J.-H. Zhao, X.-B. Li, Q.-D. Chen, Z.-G. Chen, and H.-B. Sun, "Ultrafast laser-induced black silicon, from micro-nanostructuring, infrared absorption mechanism, to high performance detecting devices," *Mater. Today Nano*, vol. 11, Aug. 2020, Art. no. 100078, doi: 10.1016/j.mtnano.2020.100078.

[3] B. Franta, E. Mazur, and S. K. Sundaram, "Ultrafast laser processing of silicon for photovoltaics," *Int. Mater. Rev.*, vol. 63, no. 4, pp. 227–240, May 2018, doi: 10.1080/09506608.2017.1389547.

[4] J. E. Carey, C. H. Crouch, M. Shen, and E. Mazur, "Visible and near-infrared responsivity of femtosecond-laser microstructured silicon photodiodes," *Opt. Lett.*, vol. 30, no. 14, pp. 1773–1775, Jul. 2005, doi: 10.1364/OL.30.001773.

[5] S. Huang *et al.*, "Black silicon photodetector with excellent comprehensive properties by rapid thermal annealing and hydrogenated surface passivation," *Adv. Opt. Mater.*, vol. 8, no. 7, Apr. 2020, Art. no. 1901808, doi: 10.1002/adom.201901808.

[6] T. H. R. Crawford, J. Yamanaka, G. A. Botton, and H. K. Haugen, "High-resolution observations of an amorphous layer and subsurface damage formed by femtosecond laser irradiation of silicon," *J. Appl. Phys.*, vol. 103, no. 5, Mar. 2008, Art. no. 053104, doi: 10.1063/1.2885111.

[7] M. J. Smith, Y. T. Lin, M. J. Sher, M. T. Winkler, E. Mazur, and S. Gradečak, "Pressure-induced phase transformations during femtosecond-laser doping of silicon," *J. Appl. Phys.*, vol. 110, no. 5, 2011, Art. no. 053524.

[8] X. Liu, B. Radfar, K. Chen, T. P. Pasanen, V. Vähänissi, and H. Savin, "Tailoring femtosecond-Laser processed black silicon for reduced carrier recombination combined with >95% above-bandgap absorption," *Adv. Photon. Res.*, vol. 3, no. 4, Apr. 2022, Art. no. 2100234, doi: 10.1002/adpr.202100234.

[9] T. Gimpel, S. Winter, M. Boßmeyer, and W. Schade, "Quantum efficiency of femtosecond-laser sulfur hyperdoped silicon solar cells after different annealing regimes," *Sol. Energy Mater. Sol. Cells*, vol. 180, pp. 168–172, Jun. 2018, doi: 10.1016/j.solmat.2018.03.001.

[10] B. Hartiti, A. Slaoui, J. C. M ́uller, and P. Siffert, "Thermal annealing of excimer-laser-induced defects in virgin silicon," *Mater. Sci. Eng. B*, vol. 4, nos. 1–4, pp. 257–260, Oct. 1989, doi: 10.1016/0921-5107(89)90252-3.

[11] H. Savin, M. Yli-Koski, and A. Haarahiltunen, "Role of copper in light induced minority-carrier lifetime degradation of silicon," *Appl. Phys. Lett.*, vol. 95, no. 15, Oct. 2009, Art. no. 152111, doi: 10.1063/1.3250161.

[12] A. A. Istratov, H. Hieslmair, and E. R. Weber, "Iron contamination in silicon technology," *Appl. Phys. A, Mater. Sci. Process.*, vol. 70, no. 5, pp. 489–534, May 2000, doi: 10.1007/s003390051074.

[13] S. Baumann, D. Kray, K. Mayer, A. Eyer, and G. P. Willeke, "Comparative study of laser induced damage in silicon wafers," in *Proc. IEEE 4th World Conf. Photovoltaic Energy Conf.*, May 2006, pp. 1142–1145, doi: 10.1109/WCPEC.2006.279363.

[14] J. Thorstensen and S. E. Foss, "Investigation of depth of laser damage to silicon as function of wavelength and pulse duration," *Energy Proc.*, vol. 38, pp. 794–800, Jan. 2013, doi: 10.1016/j.egypro.2013.07.348.

[15] J. Oh, H.-C. Yuan, and H. M. Branz, "An 18.2%-efficient black-silicon solar cell achieved through control of carrier recombination in nanostructures," *Nature Nanotechnol.*, vol. 7, no. 11, pp. 743–748, Nov. 2012, doi: 10.1038/nnano.2012.166.

[16] T. P. Pasanen, H. S. Laine, V. Vahanissi, K. Salo, S. Husein, and H. Savin, "Impact of standard cleaning on electrical and optical properties of phosphorus-doped black silicon," *IEEE J. Photovolt.*, vol. 8, no. 3, pp. 697–702, May 2018, doi: 10.1109/JPHOTOV.2018.2806298.

[17] R. A. Sinton and A. Cuevas, "Contactless determination of current–voltage characteristics and minority-carrier lifetimes in semiconductors from quasi-steady-state photoconductance data," *Appl. Phys. Lett.*, vol. 69, no. 17, pp. 2510–2512, Oct. 1996, doi: 10.1063/1.117723.

[18] M. Wilson *et al.*, "QSS-μPCD measurement of lifetime in silicon wafers: Advantages and new applications," *Energy Proc.*, vol. 8, pp. 128–134, Jan. 2011, doi: 10.1016/j.egypro.2011.06.113.

[19] G. Dingemans, R. Seguin, P. Engelhart, M. V. D. Sanden, and W. M. M. Kessels, "Silicon surface passivation by ultrathin Al_2O_3 films synthesized by thermal and plasma atomic layer deposition," *Phys. Status Solidi (RRL)-Rapid Res. Lett.*, vol. 4, nos. 1–2, pp. 10–12, Feb. 2010, doi: 10.1002/pssr.200903334.

[20] B. R. Tull, M. T. Winkler, and E. Mazur, "The role of diffusion in broadband infrared absorption in chalcogen-doped silicon," *Appl. Phys. A, Solids Surf.*, vol. 96, pp. 327–334, Aug. 2009, doi: 10.1007/s00339-009-5200-8.

[21] B. Franta *et al.*, "Simultaneous high crystallinity and sub-bandgap optical absorptance in hyperdoped black silicon using nanosecond laser annealing," *J. Appl. Phys.*, vol. 118, no. 22, Dec. 2015, Art. no. 225303, doi: 10.1063/1.4937149.

[22] K. Chen, T. P. Pasanen, V. Vahanissi, and H. Savin, "Effect of MACE parameters on electrical and optical properties of ALD passivated black silicon," *IEEE J. Photovolt.*, vol. 9, no. 4, pp. 974–979, Jul. 2019, doi: 10.1109/JPHOTOV.2019.2917787.

[23] P. Repo *et al.*, "Effective passivation of black silicon surfaces by atomic layer deposition," *IEEE J. Photovolt.*, vol. 3, no. 1, pp. 90–94, Jan. 2013, doi: 10.1109/JPHOTOV.2012.2210031.

[24] M. J. Kang, E. S. Hwang, M. Kim, T. S. Park, S. T. Shin, and B.-H. Cheong, "Enhancement of ultra-violet light absorption of surface-textured silicon induced by nanosecond laser irradiations," *Appl. Surf. Sci.*, vol. 530, Nov. 2020, Art. no. 147260, doi: 10.1016/j.apsusc.2020.147260.

[25] G. Scardera *et al.*, "On the enhanced phosphorus doping of nanotextured black silicon," *IEEE J. Photovolt.*, vol. 11, no. 2, pp. 298–305, Mar. 2021, doi: 10.1109/JPHOTOV.2020.3047420.

[26] R. S. Davidsen *et al.*, "Black silicon laser-doped selective emitter solar cell with 18.1% efficiency," *Sol. Energy Mater. Sol. Cells*, vol. 144, pp. 740–747, Jan. 2016, doi: 10.1016/j.solmat.2015.10.018.